

Wave packet dynamics of the matter wave field of a Bose-Einstein condensate

C. Sudheesh, S. Lakshmibala, and V. Balakrishnan*

Department of Physics, Indian Institute of Technology Madras, Chennai 600 036, India

(Dated: 23 June 2004)

Abstract

We show in the framework of a tractable model that revivals and fractional revivals of wave packets afford clear signatures of the extent of departure from coherence and from Poisson statistics of the matter wave field in a Bose-Einstein condensate, or of a suitably chosen initial state of the radiation field propagating in a Kerr-like medium.

PACS numbers: 03.65.Yz, 42.50.-p, 42.50.Dv

arXiv:quant-ph/0408071v1 11 Aug 2004

*Electronic address: sudheesh,slbala,vbalki@physics.iitm.ac.in

The evolution of a quantum wave packet subject to a confining potential is of current interest in several experimentally realizable situations. Foremost among these is the dynamics of the matter wave field of a Bose-Einstein condensate (BEC) confined by a three-dimensional optical lattice[1]. The condensate is, in general, in a coherent superposition of different atom-number states[2, 3, 4] with a repulsive interaction between the atoms. This state evolves in time in the confining potential. If the number of atoms and the number of lattice sites are both sufficiently large, the atom number distribution in each well obeys Poisson statistics to a good approximation. With increasing well depth and decreasing tunneling energy, the wells can be taken to be sufficiently isolated from each other. The atom number distribution in each well then departs from the Poisson, and significant non-classical effects manifest themselves[1]. These include squeezing and dissipation, sub-Poisson statistics, as well as revivals and fractional revivals at particular instants of time. A realistic and tractable model for the dynamics of the atoms in each well is provided by the Hamiltonian

$$H = \hbar\chi a^{\dagger 2} a^2 = \hbar\chi N(N - 1), \quad (1)$$

where a , a^\dagger and N are annihilation, creation and number operators of atoms, and χ characterizes the energy needed to overcome the inter-atomic repulsion in adding an atom to the population of the potential well.

As is well known, the formal equivalence between bosonic atoms and photons has been exploited in recent years to bring out the deep analogies between quantum optics and atom optics involving BECs[5], enabling a fruitful two-pronged approach to the problems of quantum computing. Wave packets propagating in a nonlinear optical medium display precisely the variety of non-classical features[6] mentioned above that BECs display. In particular, revivals and fractional revivals, which are now recognized to be generic features of wave packet evolution in nonlinear quantum dynamics, constitute a striking aspect of experimental observations[1] of BECs. The revival phenomenon[7, 8] has been studied in detail in diverse situations[9, 10, 11, 12, 13], including that of the dynamics of a single-mode field propagating in a Kerr-like medium. In this case the initial wave packet is a coherent state of the radiation field, and it is precisely the Hamiltonian in Eq. (1) (where the operators now refer to photons) that governs the dynamics.

The identification of clear signatures of revivals and fractional revivals helps distinguish between wave packets that obey Poisson statistics and those that obey sub-Poissonian statis-

tics, and also provides valuable information on the degree of coherence enjoyed by the system. This would also be of practical importance in quantum computation using wave packets, where logic gate operations are envisaged to be implemented at the precise instants of fractional revivals[14].

Specifying the state of a BEC in an actual experiment is not simple, and several models are extant. However, plausibility arguments may be given to support a pure state description[2] of the BEC, according to which the state at any time t has the general form

$$|\psi(t)\rangle = \sum_n \frac{b_n(t)}{\sqrt{n!}} |n\rangle, \quad (2)$$

where the expansion coefficients $b_n(t)$ are model-dependent. It is of great interest to study the departure from coherence of an initial state under time evolution governed by a hermitian but nonlinear Hamiltonian as in Eq. (1). What is required for this purpose is a model initial state that has three basic features: a precisely quantifiable, preferably tunable, degree of departure from perfect coherence, sub-Poissonian statistics (a standard deviation that is less than the mean), and phase-squeezing. All these properties are possessed by the normalized state

$$|\alpha, m\rangle = \frac{(a^\dagger)^m |\alpha\rangle}{\sqrt{\langle\alpha| a^m a^{\dagger m} |\alpha\rangle}} = \frac{(a^\dagger)^m |\alpha\rangle}{\sqrt{m! L_m(-\nu)}} \quad (3)$$

where m is a positive integer, $|\alpha\rangle$ is the standard oscillator coherent state defined by $a|\alpha\rangle = \alpha|\alpha\rangle$, $\alpha \in \mathbb{C}$, $\nu \equiv |\alpha|^2$, and L_m is the Laguerre polynomial of order m . The departure of $|\alpha, m\rangle$ from perfect coherence arises due to the addition of m atoms to $|\alpha\rangle$, a feature that becomes more pronounced with increasing m . In the context of quantum optics, in which this state has first been studied[15], $|\alpha, m\rangle$ is called an m -photon-added coherent state, and is produced in laser-atom interactions under appropriate conditions. Its non-classical features include both phase squeezing and sub-Poissonian statistics. The latter property implies that the standard deviation in the atom number N of the state behaves like $N^{\frac{1}{2}-\beta}$ rather than $N^{\frac{1}{2}}$, the exponent β being a calculable decreasing function of m .

While $|\alpha, m\rangle$ is not an eigenstate of a , it may be regarded[16] as a “nonlinear coherent state”, in the sense that it is an eigenstate of the operator $[1 - m(1 + a^\dagger a)^{-1}] a$ with eigenvalue α . The state $|\alpha, m\rangle$ can also be viewed in another way. Instead of the Fock basis $\{|n\rangle\}$, we may consider the unitarily transformed basis $\{|n, \alpha\rangle\}$ formed by the generalized coherent states $|n, \alpha\rangle = \exp(\alpha a^\dagger - \alpha^* a) |n\rangle$. (Equivalently, for a given n , $|n, \alpha\rangle$ is simply the state

$(a^\dagger - \alpha^*)^n |\alpha\rangle$, normalized to unity.) The initial state $|\psi(0)\rangle$ of the condensate can be expanded in the basis $\{|n, \alpha\rangle\}$ instead of the Fock basis. Likewise, it can be shown that, for a given m , the state $|\alpha, m\rangle$ is a superposition of the form $\sum_{n=0}^m c_n |n, \alpha\rangle$. Thus, in practice, $|\alpha, m\rangle$ is a very appropriate candidate for the initial state of the condensate.

In this paper we show that distinctive signatures of revivals and fractional revivals of the condensate are manifested in the mean values of certain basic operators pertaining to the system, and in their variances. We examine the precise manner in which the departure from coherence of the initial condensate wave function affects its subsequent dynamics, particularly at the instants of revivals and fractional revivals. The distinctions between different fractional revivals that occur in between two successive revivals are also brought out.

The matter wave field in a BEC is essentially given by the expectation value $\langle \psi(t) | a | \psi(t) \rangle$. Its real and imaginary parts are the expectation values of the hermitian combinations $(a + a^\dagger)/2$ and $-i(a - a^\dagger)/2$, which in turn correspond to the cases $\varphi = 0$ and $\varphi = -\frac{1}{2}\pi$ of the field quadrature $\xi = (a e^{i\varphi} + a^\dagger e^{-i\varphi})/2$ that is customarily taken[15] as the basic observable in the quantum optics context. We therefore set $x = (a + a^\dagger)/2^{1/2}$ and $p = -i(a - a^\dagger)/2^{1/2}$ (so that $[x, p] = i$), and examine the expectation values and variances of x and p as the system evolves from the initial state in Eq. (3) under the Hamiltonian H of Eq. (1). We shall see that the time dependence of these mean values and the corresponding variances mirrors, in distinct ways, the occurrence of different fractional revivals between two successive revivals of the initial state. We use the convenient notation

$$\langle x(t) \rangle_m = \langle \alpha, m | e^{iHt/\hbar} x e^{-iHt/\hbar} | \alpha, m \rangle, \quad (4)$$

with an analogous definition for $\langle p(t) \rangle_m$. As H is diagonal in the number operator N , it follows that the mean atom number, given by[15]

$$\langle N \rangle_m = \frac{(m+1) L_{m+1}(-\nu)}{L_m(-\nu)} - 1, \quad (5)$$

remains constant in time. When $\nu = 0$, $\langle N \rangle_m$ reduces to m , as required; while for $\nu \gg m$, $\langle N \rangle_m = \nu + 2m + \mathcal{O}(\nu^{-1})$. The moments of N , and hence the sub-Poissonian statistics of the atom number, also remain unaltered in time.

It is helpful to use as a reference, for the purposes of subsequent comparison, the results that obtain in the case when $m = 0$, i.e., for an initial state that is just the coherent

state $|\alpha\rangle$ (which has, of course, a Poissonian number distribution with mean value ν). A straightforward calculation gives

$$\begin{aligned} \langle x(t) \rangle_0 &= \exp[-\nu(1 - \cos 2\chi t)] \\ &\times \{x_0 \cos(\nu \sin 2\chi t) + p_0 \sin(\nu \sin 2\chi t)\}, \end{aligned} \quad (6)$$

$$\begin{aligned} \langle p(t) \rangle_0 &= \exp[-\nu(1 - \cos 2\chi t)] \\ &\times \{p_0 \cos(\nu \sin 2\chi t) - x_0 \sin(\nu \sin 2\chi t)\}. \end{aligned} \quad (7)$$

Here $\alpha = (x_0 + ip_0)/2^{1/2}$ so that $\nu = |\alpha|^2 = \frac{1}{2}(x_0^2 + p_0^2)$. The parameters x_0 and p_0 signify (in the case at hand, namely, for $m = 0$) the locations of the centers of the initial Gaussian wave packets in position and momentum space, respectively. It is evident that $\langle x(t) \rangle_0$ and $\langle p(t) \rangle_0$ are periodic in t , with a period $\pi/\chi = T_{\text{rev}}$, the revival time. (For the Hamiltonian in Eq. (1), T_{rev} coincides with the ‘‘classical orbit time’’ T_{cl} because the coefficients of the terms linear and quadratic in N happen to be equal in magnitude.) In fact, at the level of expectation values, this case can be cast in the form of a classical nonlinear oscillator with ‘‘dynamical variables’’ $X_0 \equiv \langle x(t) \rangle_0 \exp[\nu(1 - \cos 2\chi t)]$ and $P_0 \equiv \langle p(t) \rangle_0 \exp[\nu(1 - \cos 2\chi t)]$: setting $z_0(t) = \exp(i\nu \sin 2\chi t)$, Eqs. (6) and (7) become

$$\begin{aligned} X_0(t) &= x_0 \text{Re } z_0(t) + p_0 \text{Im } z_0(t), \\ P_0(t) &= p_0 \text{Re } z_0(t) - x_0 \text{Im } z_0(t). \end{aligned} \quad (8)$$

If we now *re-parametrize* time according to $\tau = \sin 2\chi t$, we have $dX_0/d\tau = \nu P_0$ and $dP_0/d\tau = -\nu X_0$. Thus, formally, we have essentially a nonlinear oscillator of frequency $\frac{1}{2}[X_0^2(0) + P_0^2(0)]$, $X_0(0)$ and $P_0(0)$ being the initial values of $X_0(\tau)$ and $P_0(\tau)$, respectively.

The time dependence of $\langle x(t) \rangle_m$ and $\langle p(t) \rangle_m$ for $m \neq 0$ differs in striking ways from the foregoing, even for small values of m . The revival time T_{rev} remains equal to π/χ , of course, but in the intervals between revivals the time evolution is considerably more involved than the expressions in Eqs. (6) and (7) for the case $m = 0$. This implies that even a small departure from coherence in the initial state of the condensate and from Poissonian number statistics leads to a very different time evolution of the system and the phase squeezing it exhibits. We have calculated the exact expressions for $\langle x(t) \rangle_m$ and $\langle p(t) \rangle_m$, and these are as follows. Their initial values are given by

$$\langle x(0) \rangle_m = \frac{L_m^{(1)}(-\nu)}{L_m(-\nu)} x_0, \quad \langle p(0) \rangle_m = \frac{L_m^{(1)}(-\nu)}{L_m(-\nu)} p_0, \quad (9)$$

where $L_m^{(1)}(-\nu) = dL_{m+1}(-\nu)/d\nu$ is an associated Laguerre polynomial. Analogous to (X_0, P_0) , let us define

$$\begin{aligned} X_m(t) &= \langle x(t) \rangle_m \exp[\nu(1 - \cos 2\chi t)], \\ P_m(t) &= \langle p(t) \rangle_m \exp[\nu(1 - \cos 2\chi t)]. \end{aligned} \quad (10)$$

The solutions for these quantities may then be written in the compact and suggestive form

$$\begin{aligned} X_m(t) &= x_0 \operatorname{Re} z_m(t) + p_0 \operatorname{Im} z_m(t), \\ P_m(t) &= p_0 \operatorname{Re} z_m(t) - x_0 \operatorname{Im} z_m(t), \end{aligned} \quad (11)$$

where

$$z_m(t) = \frac{L_m^{(1)}(-\nu e^{2i\chi t})}{L_m(-\nu)} \exp[i(2m\chi t + \nu \sin 2\chi t)]. \quad (12)$$

A number of differences between these results and those for the case $m = 0$ are noteworthy. First, $|z_m|$ varies with t , in contrast to $|z_0(t)| \equiv 1$. (Note also that $z_m(0) = L_m^{(1)}(-\nu)/L_m(-\nu) \neq 1$.) The time dependence of X_m and P_m involves the sines and cosines of the set of arguments $(2\chi lt + \nu \sin 2\chi t)$ where $l = m, \dots, 2m$. Thus, not only are “higher harmonics” present, but the arguments also involve *secular* (linear) terms in t added to the original $\nu \sin 2\chi t$. This important difference precludes the possibility of subsuming the time dependence into that of an effective nonlinear oscillator by means of a re-parametrization of the time, unlike the case $m = 0$.

We present the rest of our results with the help of figures based on numerical computation. In what follows, we set $\chi = 5$ for definiteness, and also restrict ourselves to the case $x_0 = p_0$ (there is no significant loss of generality as a result of this symmetric choice of parameters). The presence of the overall factor $\exp[-\nu(1 - \cos 2\chi t)]$ in the expressions for $\langle x(t) \rangle_m$ and $\langle p(t) \rangle_m$ implies that, for sufficiently large values of the parameter ν , the expectation values remain essentially static around the value zero, and burst into rapid variation only in the neighborhood of revivals. Smaller values of ν enable us to resolve the details of the time variation more clearly.

Figures 1(a) and (b) are, respectively, plots of the expectation values $\langle x(t) \rangle_0$ and $\langle x(t) \rangle_{10}$ versus t (in units of T_{rev}) for parameter values $x_0 = p_0 = 1$ (i.e., for $\nu = 1$). The revivals at integer values of t/T_{rev} are manifest. With increasing m (or a decreasing degree of coherence in the initial state), the relatively smooth behavior of $\langle x(t) \rangle_0$ gives way to increasingly rapid

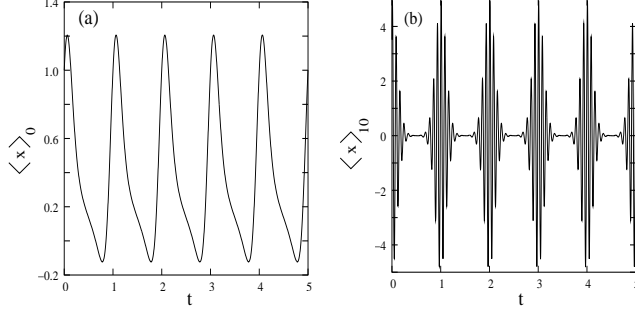


FIG. 1: $\langle x(t) \rangle_0$ as a function of time

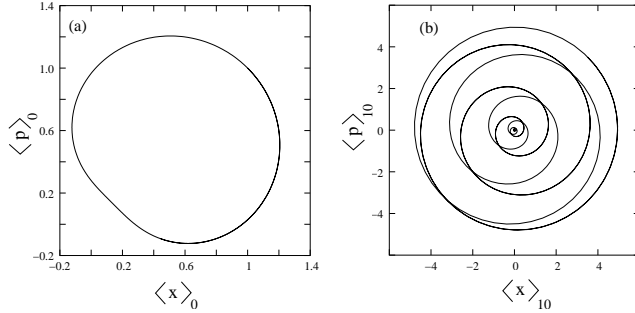


FIG. 2: “Phase plot” of $\langle p \rangle$ vs $\langle x \rangle$

oscillatory behavior in the vicinity of revivals. The range over which the expectation value varies also increases for larger values of m . Essentially the same sort of behavior is shown by $\langle p(t) \rangle_m$. However, a “phase plot” of $\langle p(t) \rangle_m$ versus $\langle x(t) \rangle_m$ in Figs. 2(a) and (b) reveals complementary aspects of such oscillatory behavior with increasing m , showing how the oscillations in the two quantities go in and out of phase with each other. (The entire closed curve in each case is traversed in a time period T_{rev} .)

The initial state also undergoes fractional revivals in the interval between any two successive revivals. In principle, it can be shown that, in the interval $(0, T_{\text{rev}})$, fractional revivals occur at the instants T_{rev}/k where $k = 2, 3, \dots$, and also, for any given k , at the instants $j T_{\text{rev}}/k$ where $j = 1, 2, \dots, (k-1)$. These fractional revivals are signaled by the appearance of k spatially-distributed wave packets similar to the wave packet representing the state at $t = 0$. The fractional revivals at the instants $j T_{\text{rev}}/k$ show up in the rapid pulsed variation of the k^{th} moments of x and p , and not in the lower moments[17]. However, if we use $|\alpha, m\rangle$ as the initial state, then, even for relatively small values of m , the signatures of fractional revivals appear for values of ν that are not large, in contrast to what happens when the initial state is the coherent state $|\alpha\rangle$. (Recall that $\langle N \rangle_m$ is determined by ν according to

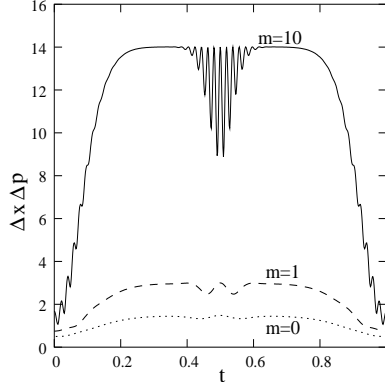


FIG. 3: Variation of the uncertainty product with time

Eq. (5).)

For illustrative purposes we investigate the specific case of the fractional revival at $t = \frac{1}{2}T_{\text{rev}}$. This corresponds to the appearance of two spatially separated similar wave packets, i.e., a single qubit in the language of logic gate operations. Plots of the product $\Delta x \Delta p$ of the standard deviations of x and p versus t/T_{rev} over a full cycle are shown in Fig. 3 for initial states given, respectively, by the coherent state $|\alpha\rangle$ (dotted curve), the atom-added state $|\alpha, 1\rangle$ (dashed curve), and the multi-atom-added state $|\alpha, 10\rangle$ (bold curve), for the same parameter values as above ($\chi = 5$, $x_0 = p_0 = 1$, so that $\nu = 1$.) It is seen that hardly any trace of the fractional revival is evident in the case of an initially coherent state, in marked contrast to the case of the atom-added states, in which the fractional revival is signaled by oscillations whose frequency and amplitude increase quite rapidly with increasing m . This effect gets masked for larger values of the parameter ν , when these oscillations are relatively insensitive to the value of m .

Another striking feature that provides a clear distinction between the revivals at $t = n T_{\text{rev}}$ and the fractional revivals at $t = (n + \frac{1}{2}) T_{\text{rev}}$ is illustrated in Fig. 4 (a), which is a plot of Δp versus Δx . The dotted and full lines correspond to $m = 0$ and $m = 5$, respectively. At $t = 0$, these quantities are equal, and have small values. As t increases, they rapidly build up, oscillating about the radial $\Delta p = \Delta x$ line with an initially increasing, and then decreasing, amplitude. A maximum value of Δx and Δp is attained, at which these quantities then remain nearly static, till the onset of the fractional revival at T_{rev} . They then begin to oscillate rapidly once again, but this time in a *tangential* direction, swinging back and forth along an arc with an amplitude that initially increases and then decreases to zero:

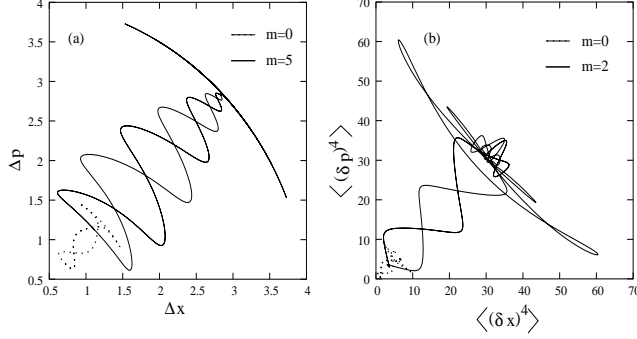


FIG. 4: “Phase plots” of higher moments of p and x

in other words, the individual standard deviations fluctuate rapidly in the vicinity of the fractional revival (while $[(\Delta x)^2 + (\Delta p)^2]^{1/2}$ remains essentially unchanged in magnitude), in marked contrast to what happens at a revival. It is evident that all these features are very significantly enhanced and magnified for non-zero values of m , relative to what happens for the case $m = 0$.

Similar signatures of fractional revivals for higher values of k can be discerned by using initial states $|\alpha, m\rangle$ even with relatively small values of ν , the oscillations in the moments of observables becoming more pronounced with increasing m . For instance, signatures of the fractional revivals at $t = \frac{1}{4}j T_{\text{rev}}$, $j = 1, 2, 3$ are clearly discernible in the behavior of the fourth moments of x . Figure 4 (b) is a plot of $\langle(\delta p)^4\rangle$ versus $\langle(\delta x)^4\rangle$ where $\delta x = x - \langle x \rangle$, $\delta p = p - \langle p \rangle$, for $\nu = 1$. The dotted and full lines correspond to the initial states $|\alpha\rangle$ and $|\alpha, 2\rangle$ respectively. Once again, the magnification of the variations that occurs for even a small value of m is manifest.

In conclusion, we have demonstrated that an atom-added initial state of the form $|\alpha, m\rangle$ shows significantly increased sensitivity to revivals and fractional revivals. In this sense, one may therefore expect that the inevitable departure, in practice, of the initial state of a BEC from perfect coherence can in fact be used to advantage.

We thank P. K. Panigrahi for discussions. This work was supported in part by the Department of Science and Technology, India, under Project No. SP/S2/K-14/2000.

-
- [1] See, e.g., M. Greiner, O. Mandel, T. W. Hänsch, and I. Bloch, *Nature* **419**, 51 (2002).
 [2] E. M. Wright, D. F. Walls, and J. C. Garrison, *Phys. Rev. Lett.* **77**, 2158 (1996).

- [3] A. Imamoglu, M. Lewenstein, and L. You, Phys. Rev. Lett. **78**, 2511 (1997).
- [4] Y. Castin and J. Dalibard, Phys. Rev. A **55**, 4330 (1997).
- [5] K. Mølmer, New J. Phys. **5**, 55.1 (2003).
- [6] See, e.g., D. F. Walls, Nature (London) **280**, 451 (1979).
- [7] For a recent review of revivals of wave packets see R. W. Robinett, Phys. Rep. **392**, 1 (2004).
- [8] J. Parker and C. R. Stroud, Jr., Phys. Rev. Lett. **56**, 716 (1986); I. Sh. Averbukh and N. F. Perelman, Phys. Lett. A **139**, 449 (1989). R. Bluhm and V. A. Kostelecky, Phys. Rev. A **50**, R4445 (1994).
- [9] M. Kitagawa and Y. Yamamoto, Phys. Rev. A **34**, 3974 (1986).
- [10] B. Yurke and D. Stoler, Phys. Rev. Lett. **57**, 13 (1986); G. J. Milburn and C. A. Holmes, *ibid.* **56**, 2237 (1986); W. Schleich, M. Pernigo, and F. L. Kien, Phys. Rev. A **44**, 2172 (1991); V. Buzek, H. Moya-Cessa, P. L. Knight and S. J. D. Phoenix, *ibid.* **45**, 8190 (1992).
- [11] K. Tara, G. S. Agarwal, and S. Chaturvedi, Phys. Rev. A **47**, 5024 (1993).
- [12] S. Seshadri, S. Lakshmibala, and V. Balakrishnan, Phys. Lett. A **256**, 15 (1999).
- [13] S. Seshadri, S. Lakshmibala, and V. Balakrishnan, J. Stat. Phys. **101**, 213 (2000).
- [14] M. Spanner, E. A Shapiro, and M. Ivanov, Phys. Rev. Lett **92**, 093001 (2004).
- [15] G. S. Agarwal and K. Tara, Phys. Rev. A **43**, 492 (1991).
- [16] S. Sivakumar, J. Phys. A: Math. Gen. **32**, 3441 (1999).
- [17] C. Sudheesh, S. Lakshmibala, and V. Balakrishnan, Phys. Lett. A **329**, 14 (2004).